WRFPM 2017
2017 Water Reactor Fuel Performance Meeting

2017 Water Reactor Fuel Performance Meeting
September 10 (Sun) ~ 14 (Thu), 2017
Ramada Plaza Jeju • Jeju Island, Korea

FUEL BEHAVIOR ANALYSIS FOR ACCIDENT TOLERANT FUEL WITH SiC CLADDING USING ADAPTED FEMAXI-7 CODE

Noriko Shirasu[1], Hiroaki Saito[1], Shinichiro Yamashita[1], Fumihisa Nagase[1]

[1] *Nuclear Science and Engineering Center, Japan Atomic Energy Agency (JAEA), Ibaraki, Japan*

ABSTRACT: *Silicon carbide (SiC) is an attractive candidate of accident tolerant fuel (ATF) cladding material because of its high chemical stability, high radiation resistance and low neutron absorption. FEMAXI-ATF has been developed to analysis SiC cladding fuel behaviors. The thermal, mechanical and irradiation property models were implemented to FEMAXI-7, which is a fuel behavior analysis code being developed in JAEA. Fuel rod behavior analysis was performed under typical boiling water reactor (BWR) operating conditions with a model based on a 9×9 BWR fuel (Step III Type B), in which the cladding material was replaced from Zircaloy to SiC. The SiC cladding shows large swelling by irradiation. It increases the gap size and decreases cladding thermal conductivity. The Young's modulus of SiC is about three times higher than that of Zircaloy. The creep rate of SiC is very low. The mechanism of relaxation of stress is also different from the Zircaloy cladding. The experimental data for SiC materials are still insufficient to construct the models, especially for evaluating fracture behavior.*

KEYWORDS: *ATF, SiC, cladding, FEMAXI-7.*

I. INTRODUCTION

After the Fukushima Daiichi Nuclear Power Station accident in 2011, enhancing the accident tolerance of light water reactors (LWRs) became more important than previous and a promising concept is the development of accident tolerant fuel (ATF)[1-3]. Silicon carbide (SiC) is an attractive candidate of ATF cladding material because of its high chemical stability under normal and accidental conditions, high radiation resistance and low neutron absorption. Since reaction between the SiC and steam is evaluated to be far inactive than that of the Zircaloy and steam, the generation of heat and hydrogen gas would be extremely suppressed[4].

The SiC has been studied as a nuclear material such as TRISO fuel for VHTR (Very High Temperature Reactors)[5]. Although monolithic Chemical Vapor Deposited (CVD) SiC show low corrosion rates, the mechanical property of the CVD SiC having tubular shape does not ensure the structural integrity. The SiC/SiC composites are also considered for the application as nuclear fuel cladding materials because of their pseudo-elastic mechanical behavior. In recent years, various multilayer SiC cladding designs have been proposed the unique features, which include corrosion protection, improvement mechanical properties and leak-tightness[6].

FEMAXI-ATF code has been developed in JAEA to analyze the SiC cladding fuel behaviors as an extended version of FEMAXI-7 code[7]. The thermal, mechanical and irradiation property models of SiC were newly implemented to the FEMAXI-7. Fuel rod behavior analysis were performed under the typical boiling water reactor (BWR) operating conditions with a model based on a 9×9 BWR fuel (Step III Type B) for identifying the difference between Zircaloy-base and SiC-base cladding. The R&D subjects on utilization of SiC as for LWR fuel cladding were prioritized from the present analysis.

II. FUEL ROD BEHAVIOR ANALYSIS

II.A. Implementation of SiC Material Properties to FEMAXI-7 Code

The thermal, mechanical and irradiation property models of SiC were implemented to FEMAXI-7 to enable the analysis of SiC cladding fuel behavior.

II.A.1. Thermal Properties

Silicon carbide shows rapid degradation of thermal conductivity and large swelling by neutron irradiation[5]. The thermal conductivity of unirradiated SiC is higher than that of Zircaloy, however, the thermal conductivity of irradiated SiC (2% swelling) decreases to about 8 W/m·K (Ref. 5), which is about half of that of Zircaloy at 300 ºC (Ref. 8). It is important to estimate the thermal conductivity of irradiated SiC. The thermal conductivity model was obtained from the relation of thermal conductivity, irradiation dose and swelling[5].The thermal conductivity is expressed as

$$\lambda = 1/\left(0.0595 \cdot S_{irr} \cdot 100 + 0.005\right) \quad (1)$$

where, λ=thermal conductivity(W/m/K), S_{irr}=volume swelling strain (described later).

Katoh et al. measured the thermal expantion of SiC/SiC and CVD SiC (Ref. 9). The samples exhibited the same linear thermal expansion behavior with no detectable differences between the composites and CVD SiC. The thermal expansion equation is expressed as[9],

$$\alpha = \left(-0.7765 + 1.4350\times10^{-2}T - 1.2209\times10^{-5}T^2 + 3.8289\times10^{-9}T^3\right)\times10^{-6} \quad (2)$$
$$\left(293K < T < 1273K\right)$$

where, α=linear expansion coefficient ((ΔL/L)/K), T=temperature (K)

The effect of neutron irradiation on the specific heat of SiC was negligibly small[10]. The specific heat of SiC is therefore assumed to be unchanged by neutron irradiation. The specific heat of SiC/SiC composite is very similar with CVD SiC. The specific heat, Cp (in J/kg K), can be approximately expressed as[5]

$$Cp = 925.65 + 0.3442T - 7.9259\times10^{-5}T^2 - 3.1946\times10^{7}/T^2 \quad (3)$$

II.A.2. Mechanical Properties

The Young's modulus at elevated temperatures has been empirically expressed by

$$E = E_0 - BT\exp\left(-\frac{T_0}{T}\right) \quad (4)$$

where B and T_0 are constants characteristic of the material in units of GPa/K and K, respectively. An elastic modulus at 0 K is expressed as E_0 (=247 GPa). Snead et al. give the constants: 0.04 GPa/K and T_0 = 962 K, by fitting the eq.(4).

The dose dependent of Young's modulus is expressed as a function of volume swelling strain, S_{irr} (Ref. 5).

$$E/E_0 = 1 - 6.974\cdot S_{irr} \quad (5)$$

Transient swelling behavior of CVD SiC has been given by the following equation by Katoh et al.[9]:

$$\dot{S}_{irr} = k_s \cdot \gamma^{\frac{1}{3}} \cdot \exp\left(-\frac{\gamma}{\gamma_{SC}}\right) \quad (6)$$

$k_s = 0.10612 - 1.5904\times10^{-4}T + 6.0631\times10^{-8}T^2$

$\gamma_{sc} = 0.51801 - 2.7651\times10^{-3}T + 9.4807\times10^{-6}T^2 - 1.3095\times10^{-8}T^3 + 6.7221\times10^{-12}T^4$ (473 K < T < 1073 K)

where $\dot{S}_{irr}$ denotes swelling rate((ΔV/V)/dpa), k_s the rate constant for swelling, γ the fast fluence (dpa), and γ_{sc} the characteristic fluence for swelling saturation by the negative feedback mechanism (dpa).

Figure 1 shows the temperature and dose dependence of volume swelling strain calculated using the adopted models, and Fig. 2 shows the sum of volume swelling strain and thermal expansion (Eq. (2)). The swelling decreases with increasing temperature.

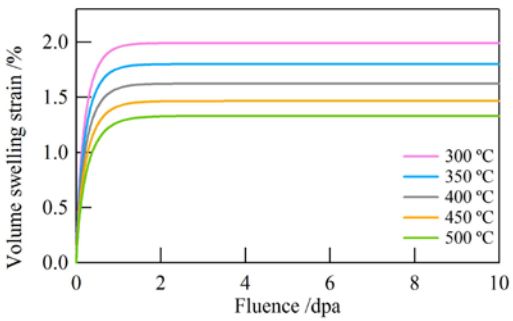

Fig. 1. Temperature and dose dependence of volume swelling strain swelling.

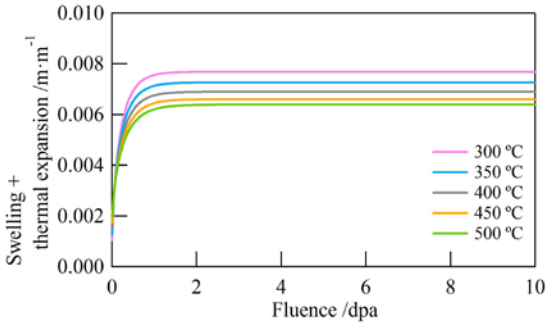

Fig. 2. Temperature and dose dependence of volume swelling + thermal expansion.

The Steady-state creep are given by Sneed et al.[5]:

$$\dot{\varepsilon} = 2\times10^{3}\left(\frac{\sigma}{191\times10^{3}}\right)^{2.3}\cdot\exp\left(-\frac{174\times10^{3}}{8.314T}\right)+2.7\times10^{-35}\sigma\phi \qquad (7)$$

where $\dot{\varepsilon}$ is creep rate (1/s), σ is applied stress (MPa), ϕ is fast neutron fluence (n/cm^2/s). The creep rate of SiC cladding is negligibly low.

Figure 3 shows the engineering stress versus strain for expanding plug testing for monolithic SiC (Hexoloy) and SiC/SiC composites[11]. The behavior of composite material is different from monolithic. Monolithic SiC has the linear relationship between strain and stress and behaves elasticly until failure. For SiC/SiC composites, the effective stress state deviates from elastic behavior near the proportional limit stress, and shows pseudo-ductility. The pseudo-ductility model for composite was developed based on the data of Fig. 3. The pseudo-ductility of SiC/SiC LWR and SiC/SiC EM^2 are expressed as

$$\sigma = 6.01\times10^{9}\,\varepsilon^{0.495} \quad \text{(SiC/SiC LWR)} \qquad (8)$$

$$\sigma = 5.035\times10^{9}\,\varepsilon^{0.487} \quad \text{(SiC/SiC EM}^2\text{)} \qquad (9)$$

where σ is true stress (N/m^2) and ε is strain. The stress-strain curves described by Eqs. (8) and (9) are shown in Fig. 4.

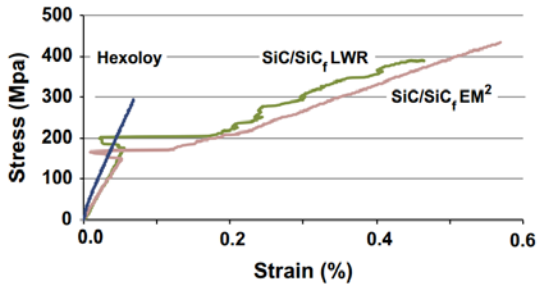

Fig. 3. Engineering stress versus strain for expanding plug testing[11].

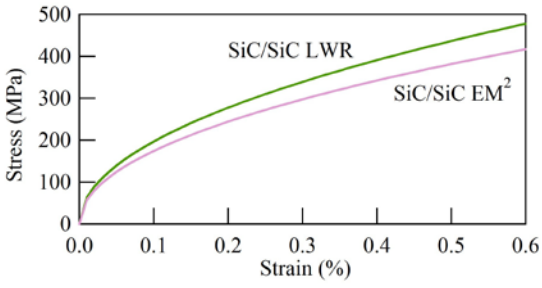

Fig. 4. Stress-strain curve discribed by Eqs.(8) and (9)

II.A.3. Other Adaptation for SiC Cladding Fuel Behavior Analysis

The FEMAXI-7 code was improved to be able to treat triplex cladding structure. The elements for thermal analysis, rod length mechanical analysis and local mechanical analysis were divided into three layers to treat the triplex structure.

The SiC cladding is corroded by coolant water and wall-thinning occur. The code was enhanced to be able to take into account the thinning behavior in outer-layer of cladding. In this study, 0.005 μm/d was used as corrosion rate[12].

II.B. Analysis Condition

We carried out a fuel rod behavior analysis under typical boiling water reactor (BWR) operating condition with a model based on a 9×9 BWR fuel (Step III Type B), in which cladding material was replaced from Zircaloy to SiC, using FEMAXI-ATF code. The fuel behavior analysis for Zircaloy cladding with same geometry also performed for the comparison. The triplex SiC cladding consist of three layers of monolithic SiC, SiC/SiC composite and monolithic SiC is used for the analysis. Calculation condition for fuel rod analysis is shown in Table 1. The axial power distribution is assumed to be a 20-step chopped cosine profile with a peaking factor of 1.4, as depict in Fig. 5. The burnup and power history are shown in Figs. 6 and 7.

Table 1. Calculation condition for fuel rod analysis

Reactor Type	BWR 9x9 step III type B
Pellet	
Diameter (cm)	1.10
Density (%TD)	97
U-enrichment (%)	3.7
Burnup (avg.) (GWd/t)	45
Cladding	
Material	SiC/SiC composite, monolithic SiC
Inner diameter (cm)	1.10
Thickness (cm)	0.070
Inner layer (monolithic SiC) (cm)	0.032
Middle layer (SiC/SiC composite) (cm)	0.034
Outer layer (monolithic SiC) (cm)	0.004
Fuel rod	
Fill gas pressure (MPa)	1.0 (He)
Plenum volume (cm^3)	21.53
Stack length (cm)	371.0
Diametral gap size (cm)	0.02

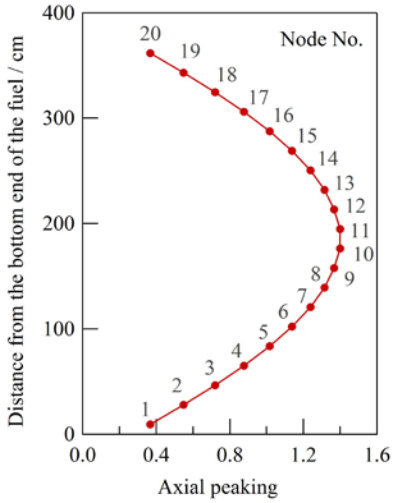

Fig. 5. Axial power distribution

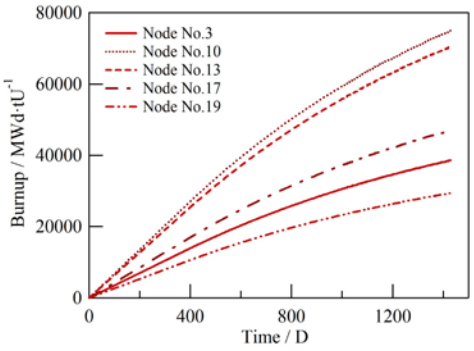

Fig. 6. Burn-up

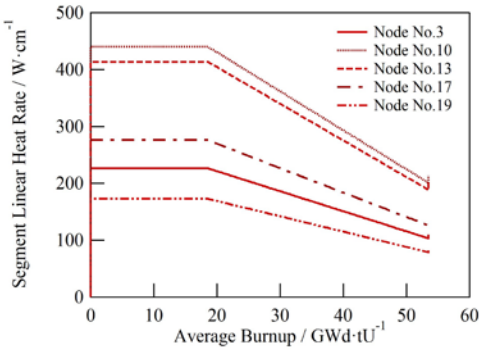

Fig. 7. Power history

III. RESULTS AND DISCUSSION

III.A. Thermal Behavior

Fuel center temperature, fuel surface temperature and cladding inner surface temperature are shown in Figs. 8, 9 and 10, respectively. The fuel surface temperature of SiC cladding fuel reaches around 1300 ºC. The temperature is much higher than that of Zircaloy cladding fuel. Consequently, the fuel center temperature of SiC cladding fuel is very high: it is around 2500 ºC. One reason is the degradation of SiC thermal conductivity by irradiation damage (Fig. 11), and another reason is the swelling behavior. The radial No.1, 4, 8 indicate inner-side of cladding, center of cladding and outer-side cladding, respectively, in Fig. 11. Figure 12 show pellet-clad gap size change. In water reactors with Zircaloy cladding, pellet-clad gap size decreases at an early stage of irradiation due to cladding creep-down, and the gap is closed. However, the gap size of SiC cladding fuel is larger than that of Zircaloy cladding fuel, and the gap is not closed during irradiation due to the swelling of cladding by irradiation. The low gap thermal conductance of SiC cladding fuel causes the increase the fuel temperature and high fission gas release rate (Fig. 13). In this analysis, the improvement of gap conductance due to re-relocation of pellets is not considered.

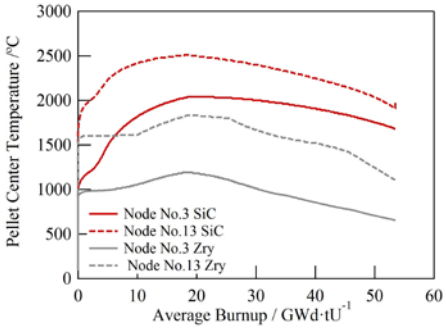

Fig. 8. Fuel center temperature

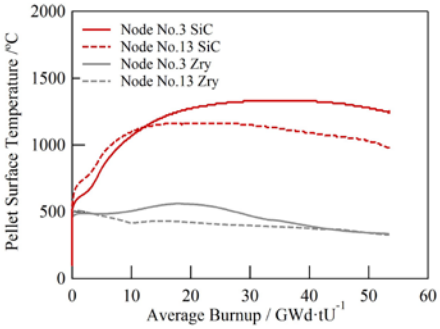

Fig. 9. Fuel surface temperature

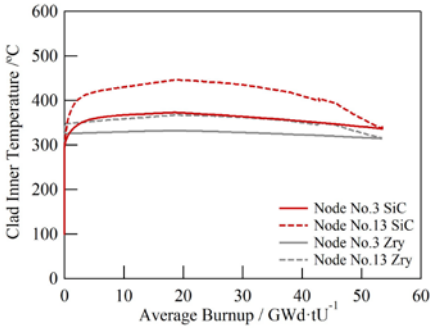

Fig. 10. Cladding inner surface temperature

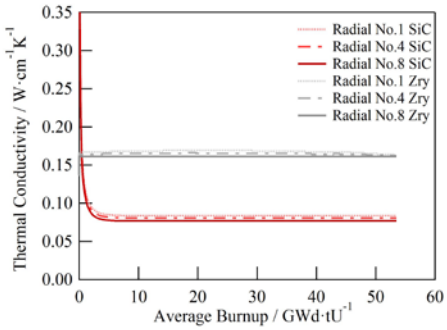

Fig. 11. Thermal conductivity (Node No.13)

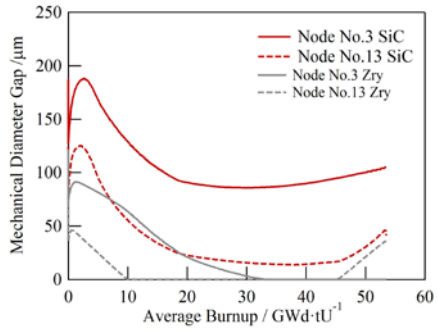

Fig. 12. Pellet-clad gap size change

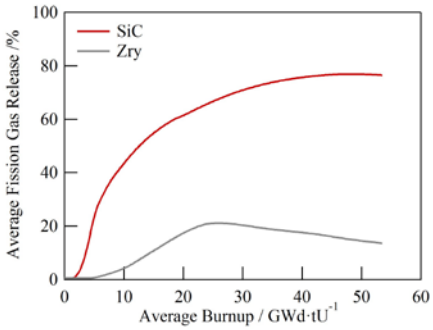

Fig. 13. Fission gas release rate

III.B. Mechanical Behavior

One of the characteristic feature of SiC is the swelling behavior. The cladding outer diameter change and volume swelling strain of SiC cladding is shown in Figs. 14 and 15. SiC shows large swelling by neutron irradiation. The swelling is higher at lower temperature. The degradation of thermal conductivity causes the increase in temperature gap between inside and outside of cladding. The SiC cladding is subjected to high stress due to the differential swelling rate. The outside of cladding is applied with compression stress. It means the tolerance for rupture owing to the PCMI decrease. The swelling

behavior and stress generation mechanism of SiC cladding are quite different from those of Zircaloy cladding. It is necessary to modify the model for SiC cladding.

Figure 16 shows the circumferential creep strain of (a) SiC and (b) Zircaloy cladding. The creep strain is more than two orders of magnitude lower than that of Zircaloy cladding. The creep behavior of SiC cladding fuel does not contribute to the deformation of cladding. Since there is no stress relaxation due to creep, the cladding circumferential stress of SiC increases with increase of inner pressure (Fig. 17).

The Young's modulus of the SiC is about three times higher than that of Zircaloy (Fig. 18). Further, the hardness of SiC cladding is higher than UO_2 pellets. The mechanism of relaxation of stress would be different from Zircaloy cladding. The failure of cladding is judged by comparing the cladding circumferential stress and ultimate tensile strength (UTS) in this analysis. We need to take in the mechanical data under irradiation for the more accurate estimation.

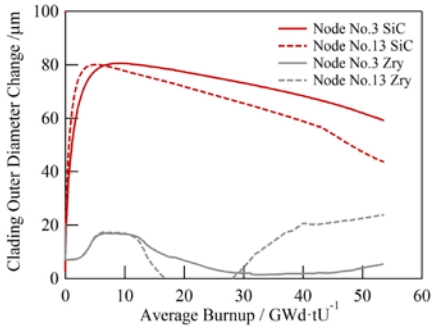

Fig. 14. Cladding outer diameter of SiC cladding fuel

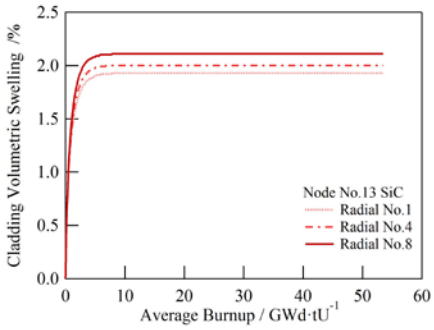

Fig. 15. Volume swelling strain of SiC cladding fuel

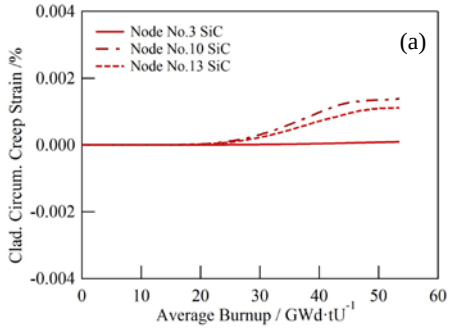

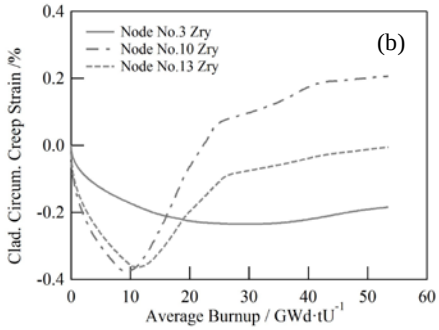

Fig. 16. Creep strain (a) SiC cladding fuel, (b) Zircaloy cladding fuel

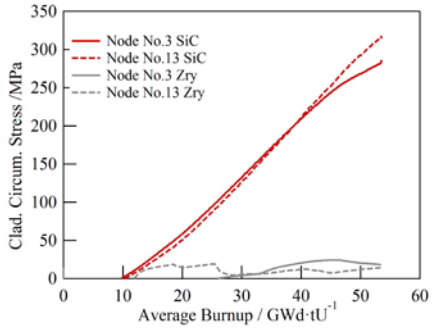

Fig. 17. Cladding circumferential stress.

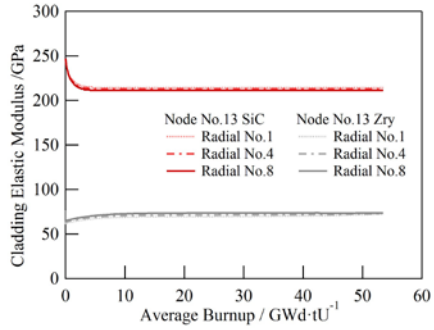

Fig. 18. Young's modulus.

III.C. Corrosion Behavior

The oxide layer thickness on outside of SiC cladding is shown in Fig. 19. The thickness indicates the thinning thickness of SiC cladding by corrosion. The thickness obtained by the analysis was about 15~28 μm. However, the corrosion rate increases with the concentration of dissolved oxygen. Furthermore, the resistance to corrosion depend on the fabrication process of SiC. The thinning of cladding has effect on cladding stress, or integrity of fuel rod. Further investigation is desirable.

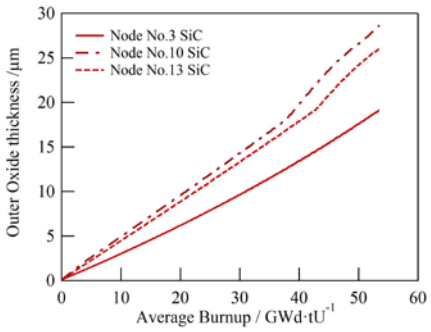

Fig. 19. Oxide thickness of outside of SiC cladding

IV. SUMMARY

The analysis using a FEMAXI-ATF code indicated that the SiC cladding shows far larger swelling by irradiation than the Zircaloy cladding, which increases the gap size and consequently increases fuel temperature and fission gas release. It is desirable to expand the property data to higher temperature range. Furthermore, the cladding swelling causes the decrease of cladding thermal conductivity, and consequently increases temperature gradient between inside and outside of cladding. The swelling decreases monotonously with increasing temperature. The SiC cladding is subjected to high stress due to the differential swelling rate. These features of swelling and stress generation of SiC cladding differ from those of Zircaloy cladding. It is necessary to modify the models for SiC cladding to improve accuracy of analysis.

The Young's modulus of the SiC is about three times higher than that of Zircaloy, and the creep rate of SiC is very low. These cause the large difference on mechanism of relaxation of stress, compared to the Zircaloy cladding. In the present stress analysis, the pseudo-ductility of SiC/SiC composite was assumed. Then, the threshold condition of cladding failure was evaluated by comparing the cladding circumferential stress and UTS. The threshold of failure became reasonably larger by introducing the pseudo-ductility. The verification of cladding rupture model is necessary by accumulating irradiated/non-irradiated mechanical data for enhancement of analysis accuracy.

ACKNOWLEDGMENTS

This study is the result of “Development of Technical Basis for Introducing Advanced Fuels Contributing to Safety Improvement of Current Light Water Reactors” carried out under the Project on Development of Technical Basis for Safety Improvement at Nuclear Power Plants by Ministry of Economy, Trade and Industry (METI) of Japan.

REFERENCES

1. US-DOE report, “Light Water Reactor Accident Tolerant Fuel Performance Metrics”, INL/EXT-13e29957, FCRS-FUEL-2013-000264., Feb. 2014.
2. Expert Group on Accident Tolerant Fuels for Light Water Reactors Mandate, Nuclear Energy Agency, Boulogne-Billancourt (France), 2014 [Internet]. Available from: https://www.oecd-nea.org/science/egatfl/.
3. S. YAMASHITA et al., “Establishment of Technical Basis to Implement Accident Tolerant Fuels and Components to Existing LWRs”, *Top Fuel 2016*, Boise, ID, September 11-15, 17550 (2016).
4. S.J. ZINKLE et al., “Accident tolerant fuels for LWRs: A perspective”, *J. Nucl. Mater*. **448** 374 (2014).
5. L.L. SNEAD et al., “Handbook of SiC properties for fuel performance modeling”, *J. Nucl. Mater.*, **371** 329 (2007).
6. Y. KATOH and K.A.TERRANI, “Systematic Technology Evaluation Program for SiC/SiC Composite-based Accident-Tolerant LWR Fuel Cladding and Core Structures”: Revision 2105, ORNL/TM-2015/454.
7. M. SUZUKI et al. “Light water reactor fuel analysis code FEMAXI-7; model and structure”. JAEA-Data/Code 2013-005 (2013).

8. D.L. HAGRMAN and G.A. REYMAN, "MATPRO-Version11, A Handbook of Materials properties for use in the analysis of light water reactor fuel rod behavior", NUREG/CR-0497, TREE-1280, Rev.3 (1979).
9. Y. KATOH et al., "Continuous SiC fiber, CVI SiC matrix composites for nuclear applications: properties and irradiation effects", *J. Nucl. Mater.*, **448** 448 (2014).
10. C.W. LEE, F.J. PINEAU and J.C. CORELLI, "Thermal properties of neutron-irradiated SiC; effects of boron doping" *J. Nucl. Mater.* **108&109** 678 (1982) .
11. G.M. JAKOBSEN et al., "Investigation of the C-ring test for measuring hoop tensile strength of nuclear grade ceramic composites", *J. Nucl. Mater.*, **452** 125 (2014).
12. K.A. TERRANI et al., "Hydrothermal corrosion of SiC in LWR coolant environments in the absence of irradiation", *J. Nucl. Mater.*, **465** 488 (2015).